

Supporting information

SARS-CoV-2 Inactivation: Assessing the Efficacy of GO-Anchored Filters Versus Various Commercial Masks

Md. Saidul Islam, ^{a,b,||} Nurun Nahar Rabin, ^{a,b,||} MST Monira Begum, ^c Nonoka Goto, ^a Ryuta Tagawa, ^a Mami Nagashima, ^d Kenji Sadamasu, ^d Kazuhisa Yoshimura, ^d Junko Matsuda, ^e Yoshihiro Sekine ^{a,f} Terumasa Ikeda ^{c,*}, and Shinya Hayami ^{a,b,g,*}

^aDepartment of Chemistry, Faculty of Advanced Science and Technology, Kumamoto University, 2-39-1 Kurokami, Kumamoto 860-8555, Japan.

^bInstitute of Industrial Nanomaterials, Kumamoto University, 2-39-1 Kurokami, Chuo-ku, Kumamoto 860-8555, Japan.

^cDivision of Molecular Virology and Genetics, Joint Research Center for Human Retrovirus Infection, Kumamoto University, Kumamoto 860-0811, Japan.

^dTokyo Metropolitan Institute of Public Health, Tokyo 169-0073, Japan.

^eInternational Research Center for Hydrogen Energy, Kyushu University, 744 Motooka, Fukuoka, Fukuoka, 819-0395, Japan.

^fPriority Organization for Innovation and Excellence, Kumamoto University, 2-39-1 Kurokami, Chuo-ku, Kumamoto 860-8555, Japan.

^gInternational Research Center for Agricultural and Environmental Biology (IRCAEB) 2-39-1 Kurokami, Chuo-ku, Kumamoto 860-8555, Japan.

*Equal correspondence.

|| Equal contribution

Experimental procedure:

Characterization of commercial mask and GO anchored filters

Commercial masks were characterized using SEM and corresponding EDX measurements. Commercial PTFE filter and GO-anchored PTFE filter samples were characterized using STEM-HAADF, STEM-BF, and TEM analysis of the cross-section.

Cell line

VeroE6/TMPRSS2 cells (VeroE6 cells stably expressing human TMPRSS2; JCRB Cell Bank, JCRB1819)^[1] were maintained in 10% heat-inactivated fetal bovine serum (NICHIREI, cat# 175012)/DMEM (Wako, cat# 041-29775) containing 1 mg/mL G418 (Wako, cat# 070-06803) and 1% penicillin/streptomycin (Wako cat# 168-23191).

Plaque assay

A plaque assay was performed as described previously.^[2-8] The day before infection, 1×10^5 VeroE6/TMPRSS2 cells were seeded in a 24-well plate. Next day, 200 μ L of virus stock and 1.6 mL of serum-free virus dilution buffer [20 mM HEPES, nonessential amino acids (Thermo Fisher Scientific, cat# 11140-050) and antibiotics in $1 \times$ DMEM]. After 1 h incubation at room temperature, the virus solution was centrifuged at $22,000 \times g$ for 1 min. The supernatant was passed through the filter, commercial mask, or GO-anchored filter and serially diluted with serum-free virus dilution buffer (10- to 10,000-fold dilutions). Then, the cells were infected with 250 μ L of each diluted virus solution at 37°C. At 1 h postinfection, 500 μ L of mounting solution [$1 \times$ DMEM including 3% FBS and 1.5% carboxymethyl cellulose (Sigma, cat# C9481-500G)] was overlaid and the cells were incubated at 37 °C. After 3 days, the cells were washed with PBS three times, followed by fixation with 4% paraformaldehyde (Nacalai Tesque, cat# 09154-85). The fixed cells were washed with water, dried, and stained with 0.1% methylene blue (Nacalai Tesque, cat# 22412-14) in water. The stained cells were washed with water and dried, and the number of plaques was counted for plaque-forming unit determination.

In the plaque assay, the 1h incubation period following the dilution of the sample serves as a crucial step to allow for viral attachment and penetration into the host cells. During this time, the diluted viral sample is introduced to a monolayer of susceptible host cells, allowing the viral particles to adhere to the cell surface and subsequently enter the cells. This incubation period allows for synchronization of the infection process across the population of host cells, ensuring consistency in viral replication and plaque formation. Moreover, the incubation period allows for optimizing environmental conditions necessary for efficient viral infection, such as temperature and pH. Overall, the 1 h incubation period is pivotal in initiating the infection process and facilitating the subsequent quantification of viral titer through plaque formation.

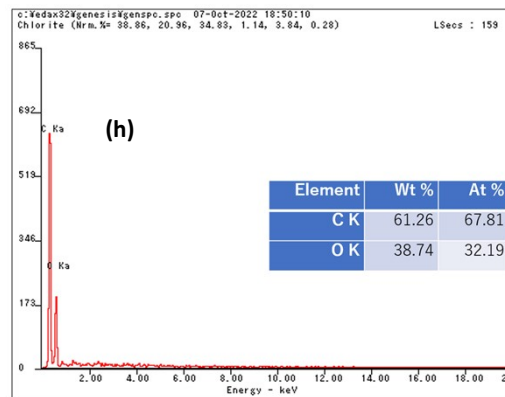
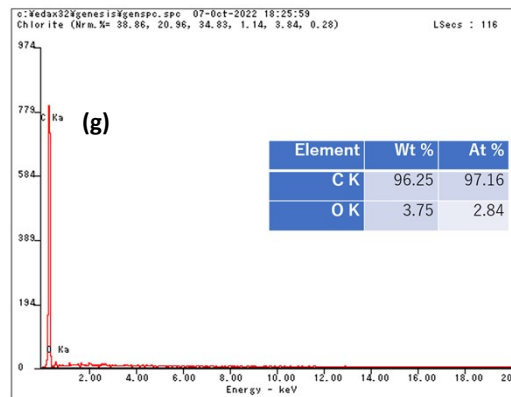
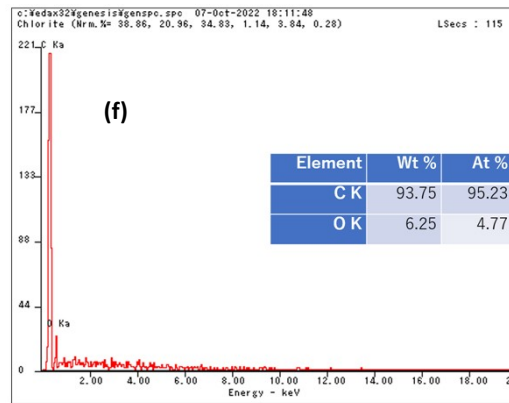
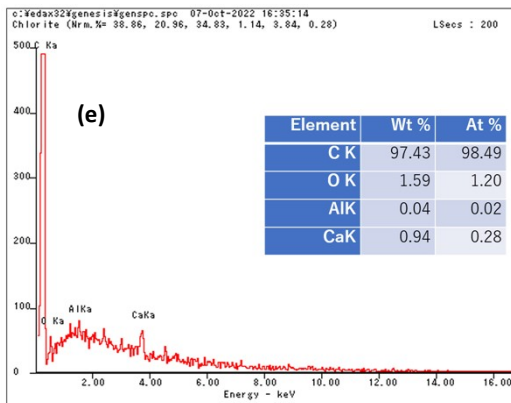
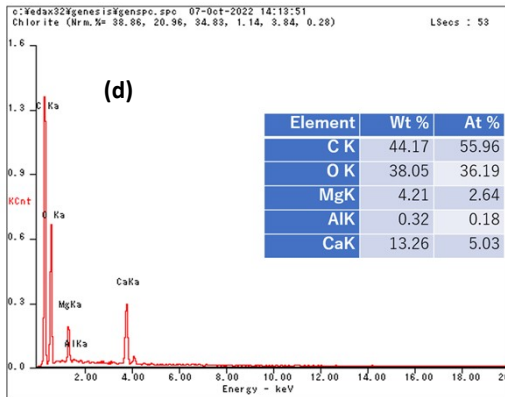
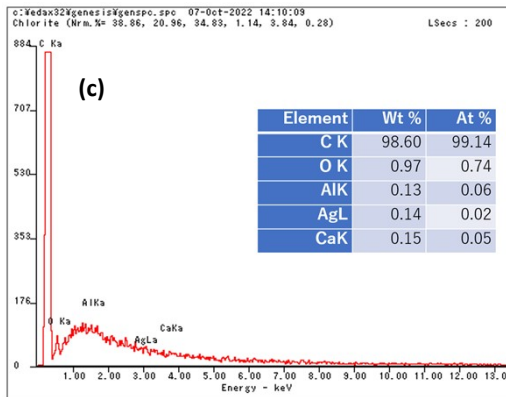
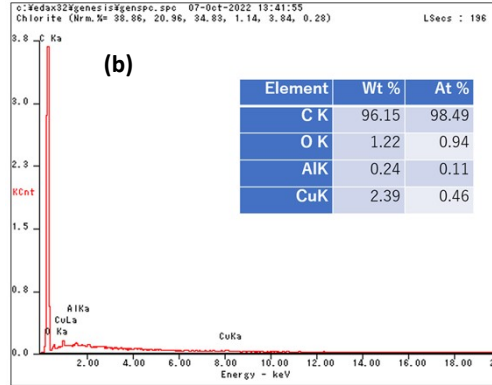
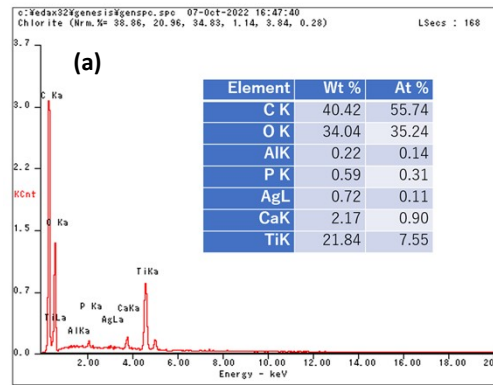


Figure S1: EDX of a. hydro silver titanium mask, b. copper oxide mask, c. silver ion ceramic mask, d. special dolomite CDM mask, e. pioneer mask, f. CLEANXIA mask, g. SHARP mask, and h. surgical mask.

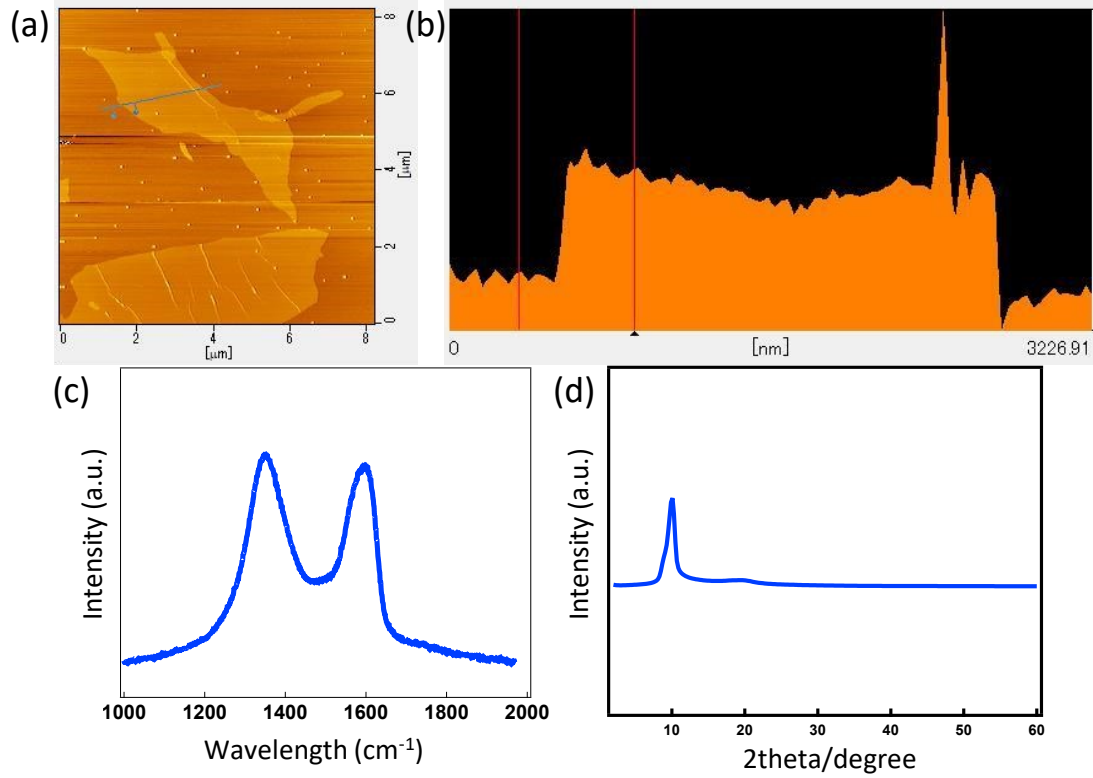


Figure S2: Characterization of GO. a) AFM image of GO, b) corresponding height profile, c) Raman spectrum of GO, and d) PXRD spectrum of GO.

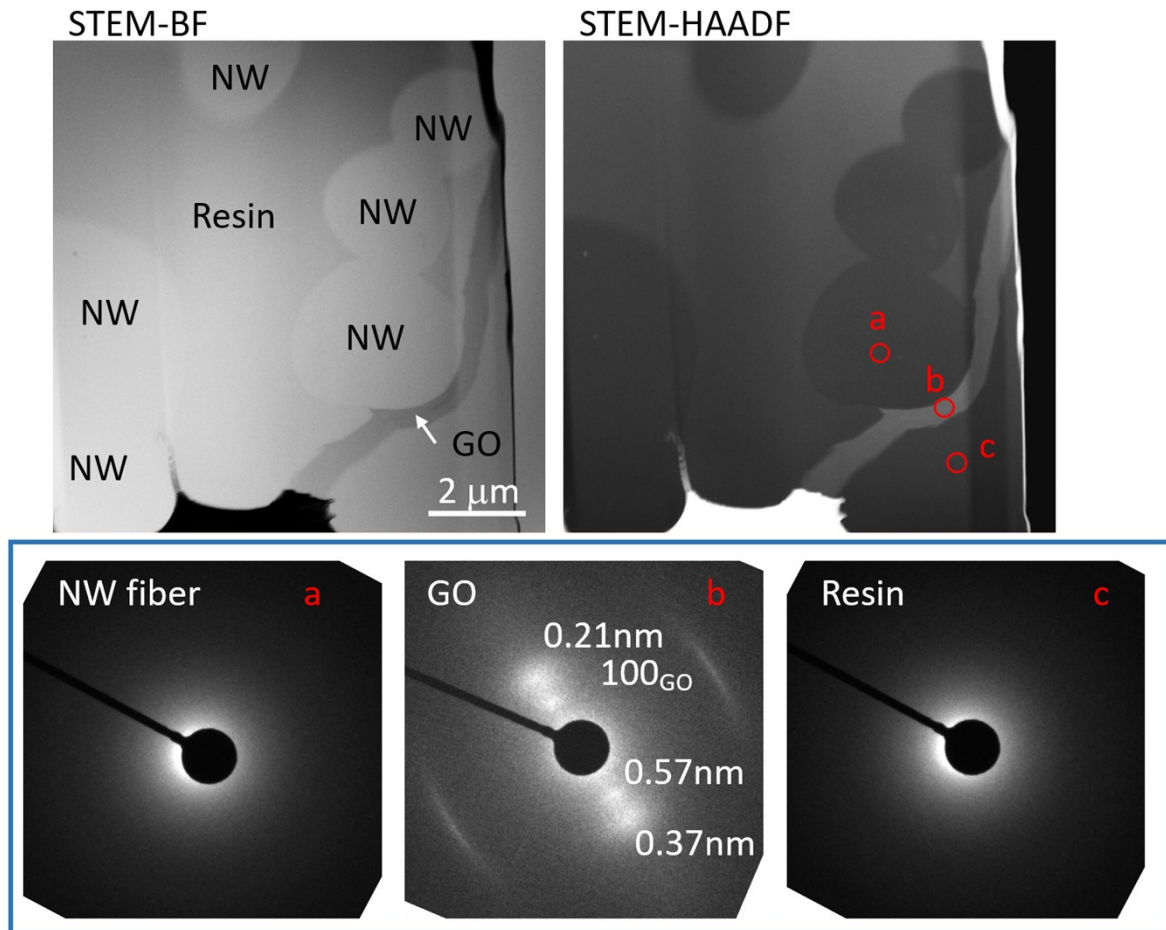


Figure S3: STEM-BF and STEM-HAADF of GO-anchored PTFE filter and corresponding selected area electron diffraction pattern.

References:

1. S. Matsuyama et al., *Proc Natl Acad Sci U S A*, 2020, 117(13), 7001-7003.
2. M. Fukuda, M. S. Islam, R. Shimizu, H. Nasser, N. N. Rabin, Y. Takahashi, Y. Sekine, L. F. Lindoy, T. Fukuda, T. Ikeda and S. Hayami, *ACS Applied Nano Materials*, 2021, 4, 11881-11887.
3. M. S. Islam, M. Fukuda, M. J. Hossain, N. N. Rabin, R. Tagawa, M. Nagashima, K. Sadamasu, K. Yoshimura, Y. Sekine, T. Ikeda and S. Hayami, *Nanoscale Advances*, 2023, 5, 2413-2417.
4. I. Kimura, D. Yamasoba, T. Tamura, N. Nao, T. Suzuki, et.al., *Cell*, 2022, 185, 3992-4007.e3916.
5. MST M. Begum, K. Ichihara, O. Takahashi, H. Nasser, M. Jonathan, K. Tokunaga, I. Yoshida, M. Nagashima, K. Sadamasu, K. Yoshimura, K. Sato, T. Ikeda, *bioRxiv*, 2023.

6. A. Saito, T. Irie, R. Suzuki, T. Maemura, H. Nasser, K. Uriu, Y. Kosugi, et al., *Nature*, 2022, 602, 300-306.
7. R. Suzuki, D. Yamasoba, I. Kimura, L. Wang, M. Kishimoto, J. Ito, Y. Morioka, et al., *Nature*, 2022, 603, 700-705.
8. D. Yamasoba, I. Kimura, H. Nasser, Y. Morioka, N. Nao, J. Ito, K. Uriu, M. Tsuda, J. Zahradnik, K. Shirakawa, et al., *Cell*, 2022, 185, 2103-2115.e2119.